HHS Public Access

Author manuscript

Oncogene. Author manuscript; available in PMC 2014 February 08.

Published in final edited form as:

Oncogene. 2013 August 8; 32(32): 3754–3764. doi:10.1038/onc.2012.383.

Coupling S100A4 to Rhotekin alters Rho signaling output in breast cancer cells

Min Chen[1,3], **Anne R. Bresnick**[2], and **Kathleen L. O'Connor**[1,3]

[1]University of Kentucky, 741 South Limestone, Lexington, KY 40506

[2]AlbertEinstein College of Medicine, 1300 Morris Park Avenue, Bronx, NY 10461

Abstract

Rho signaling is increasingly recognized to contribute to invasion and metastasis. In this study, we discovered that metastasis-associated protein S100A4 interacts with the Rho binding domain (RBD) of Rhotekin, thus connecting S100A4 to the Rho pathway. GST pull-down and immunoprecipitation assays demonstrated that S100A4 specifically and directly binds to Rhotekin RBD, but not other Rho effector RBDs. S100A4 binding to Rhotekin is calcium-dependent and uses residues distinct from those bound by active Rho. Interestingly, we found that S100A4 and Rhotekin can form a complex with active RhoA. Using RNAi, we determined that suppression of both S100A4 and Rhotekin leads to loss of Rho-dependent membrane ruffling in response to EGF, an increase in contractile F-actin "stress" fibers, and blocked invasive growth in three-dimensional culture. Accordingly, our data suggest that interaction of S100A4 and Rhotekin permits S100A4 to complex with RhoA and switch Rho function from stress fiber formation to membrane ruffling to confer an invasive phenotype.

Keywords

Rho; Rhotekin; S100A4/metastasin; lamellipodia; invasive growth

INTRODUCTION

While metastasis remains the major contributing factor to cancer-related deaths, there are few genes that specifically associate with the metastatic process. Of these genes, the calcium binding protein S100A4 is well recognized for its metastasis-associated properties. S100A4, also known as fibroblast specific protein (FSP), is upregulated during the epithelial to mesenchymal transition and is known to contribute to increased migration, invasion and

[3]Address correspondence to: Kathleen L. O'Connor, Ph.D., Markey Cancer Center, University of Kentucky, 741 S. Limestone Street, Lexington, KY 40506-0509, USA, Phone: 859-323-7534 (office), 859-323-7173 (lab), Fax: 859-323-6030, mch235@uky.edu. Min Chen, M.D., Ph.D., Markey Cancer Center, University of Kentucky, 741 S. Limestone Street, Lexington, KY 40506-0509, USA, Phone: 859-323-7173, Fax: 859-323-6030, kloconnor@uky.edu.

Supplementary Information accompanies the paper on the Oncogene website (http://www.nature.com/onc).

CONFLICT OF INTEREST:
The authors have no conflict of interest to declare.

metastasis (1). Growing evidence demonstrates that S100A4 is associated with the progression of a variety of cancers, including breast and colon (2, 3). S100A4 is released from cells such as stromal and tumor cells where it has been suggested to serve as a paracrine and/or autocrine secretion factor that can participate in multiple aspects of tumor progression (4). Intracellularly, the migratory-promoting effects are potentiated by the interaction of S100A4 with cytoskeletal proteins such as non-muscle myosin IIA. S100A4 colocalizes with myosin IIA at the leading edge of migrating cells (5) and affects myosin IIA assembly which, in turn, promotes directional cell migration (6, 7). These observations imply that S100A4 can serve as a regulator of actin cytoskeleton reorganization.

During the initial stages of tumor metastasis when cells migrate away from the primary tumor and invade the surrounding tissue, the actin cytoskeleton must be continuously and coordinately reorganized. Membrane protrusions (including lamellipodia, membrane ruffles, lamellae and filopodia), and stress fibers are important dynamic structures that are formed during actin cytoskeletal reorganization through the actions of the three best-characterized Rho GTPases including Rho, Rac and Cdc42. Among them, Rho is responsible for stress fiber formation in most cell types where it is suggested to function in the rear of the cell (8). Despite the prevailing view that RhoA functions in the rear of the cell while Rac and Cdc42 function at the leading edge, there are substantial data to support that RhoA is active at the leading edge of migrating cells and its activation actually precedes that of Rac (9). Furthermore, several studies have shown that RhoA can specifically promote membrane ruffling and facilitate cell motility, particularly in cells of epithelial origin (10–13). RhoA mediates actin stress fiber formation, as well as membrane ruffling, through ROCK and mDia pathways (14, 15). Therefore, how RhoA regulates these different aspects of actin reorganization, to switch between stress fibers and membrane ruffles, remains an important and unanswered question. In our current study, we provide evidence that the answer to this question may reside with one of Rho’s poorly understood effectors, Rhotekin.

Rhotekin is a scaffold protein that interacts with RhoA and RhoC equally well (16). The search for Rhotekin interacting proteins focused on the C-terminal domain, which contains a consensus-binding motif for class I PDZ proteins. These studies showed that Rhotekin interacts with vinexin, Lin7B, PIST and septin which function in cell polarity, focal adhesion and septin organization (17–19). Notably, Rhotekin is overexpressed in metastatic colon cancer cells (20) and gastric adenocarcinoma cells, where it confers resistance to apoptosis through activation of NF-κB (21). Despite these findings, the role of Rhotekin in Rho-mediated downstream signal transduction and actin cytoskeleton reorganization remains largely unknown.

We find that S100A4 can bind the RBD of Rhotekin. Here, we characterize the interaction of the RBD of Rhotekin with S100A4, the relationship of this complex with Rho, and dissect the biological function of this interaction on actin cytoskeletal organization and three-dimensional (3D) invasive growth of breast cancer cells. Through these studies, we provide evidence that the S100A4-Rhotekin interaction guides the switch between RhoA mediated stress fibers and membrane ruffling to facilitate a more invasive phenotype.

RESULTS

S100A4 specifically and directly interacts with Rho effector Rhotekin in a calcium-dependent manner

Rho effectors were originally classified into three groups depending on the regions of Rho to which they bind. Class I includes Rhotekin, PKN/PRK and Rhophilin; class II includes ROCKI and ROCKII; and class III contains citron (22). Based on similarities in their domain structure, Rho effectors were recategorized recently into three groups in which citron was listed as the member with ROCKI and ROCKII, while mDia was considered as a separate group (23). Rhotekin is a class I Rho effector and a scaffold protein (24) that is overexpressed in several cancers (20, 25). How Rhotekin contributes to cancer progression, however, is still uncertain. We initially observed that S100A4 precipitated with the RBD of Rhotekin while probing cell lysates for RhoA activity (data not shown). To investigate this interaction further, we chose representative effectors from each class plus mDia1 and Pak Rac/Cdc42 binding domains (PBD) and tested the ability of S100A4 to bind the GTPase binding domain of each effector. As shown in Figure 1A, S100A4 specifically interacted with RBD of Rhotekin, a class I Rho effector, but not other Rho effectors, GST or PBD.

Calcium binding to S100A4 induces a conformational rearrangement that allows the interaction of S100A4 with its target proteins (25, 26). To determine whether the interaction between S100A4 and the RBD of Rhotekin is direct and calcium regulated, bacterially-expressed Rhotekin RBD was incubated with 10 ng-1 μg of purified S100A4 in the presence of calcium or EGTA. As presented in Figure 1B, the binding of purified S100A4 to GST-Rhotekin RBD beads was abolished by EGTA. These data demonstrate that the interaction between S100A4 and Rhotekin RBD is direct and requires calcium.

The RBD of Rhotekin is located at the N-terminus. The amino acid sequence of the Rhotekin RBD shares approximately 30% identity with the RBDs of class I Rho effectors Rhophilin and the serine/threonine kinase PKN (16). To determine if S100A4 binds to other class I Rho effectors, GST-fusion proteins containing the RBD of PKN1 or Rhophilin2 were incubated with purified S100A4 protein. As shown in Figure 1C, S100A4 bound only the RBD from Rhotekin.

To confirm that the interaction of Rhotekin and S100A4 occurs *in vivo*, MDA-MB-231 cells, which express high levels of endogenous S100A4, were transfected with myc-tagged Rhotekin constructs including full-length (FL), ΔRBD, RBD, central domain (Cent) and C-terminus domain proteins as depicted in Figure 1D. Fusion proteins were immunoprecipitated with anti-myc IgG agarose beads and analyzed for S100A4 association by immunoblot analysis. We find that endogenous S100A4 immunoprecipitated with full-length or RBD-only Rhotekin fusion proteins (Fig. 1E, top panel; lane 3 and 5) but not with the C-terminus, ΔRBD, or central domains (Fig. 1E top panel; lanes 4, 6, and 7). Similarly, in MDA-MB-231 cells transfected with Flag-tagged full-length Rhotekin, C-terminus and ΔRBD proteins, S100A4 immunoprecipitated with only the Flag-tagged full-length Rhotekin. The C-terminus and ΔRBD mutants did not exhibit any interaction with S100A4 (Fig. 1F, top panel). Collectively, these data show that S100A4 directly and specifically interacts with Rhotekin through its RBD and this interaction is calcium-dependent.

S100A4 and Rhotekin co-localize in membrane ruffles at the edge of the migrating cells

In migrating cells, S100A4 is present at the leading edge (5). To evaluate whether Rhotekin and S100A4 colocalize in cells, a HA-tagged full-length Rhotekin construct (HA-RTKN-FL) was transfected into HeLa cells and the localization of S100A4 and Rhotekin was examined by confocal microscopy. As shown in Figure 2, unstimulated cells displayed a flattened morphology with large lamellar protrusions. S100A4 and Rhotekin colocalized throughout the cell and concentrated modestly at the edge of lamellipodia. In contrast, EGF-stimulated cells exhibited dramatic lamellipodial membrane ruffles. Interestingly, S100A4 and Rhotekin concentrated and colocalized in the edge of these ruffles (Fig. 2). The colocalization of these two proteins was also observed in the basal surface of the cells.

S100A4, active Rho, and Rhotekin form a complex

The ability of S100A4 to bind directly to the RBD of Rhotekin raises the question as to whether active Rho and S100A4 bind the RBD using the same residues. To test this idea, we utilized a Rhotekin RBD triple A mutant, which contains alanine substitutions at Arg37, Arg39 and Asp40, respectively, and has been demonstrated to bind GTP-bound Rho with reduced affinity (27). Comparing this mutant to the wild-type Rhotekin RBD, we found that S100A4 exhibited comparable binding to the RBD triple A mutant as to the wild-type RBD (Fig. 3A). To confirm that GTP-bound Rho exhibits reduced binding to the RBD triple A mutant, LPA-treated MDA-MB-231 cells were assayed for active RhoA. Figure 3C shows that GTP-bound RhoA exhibited reduced binding for Rhotekin RBD triple A mutant compared to the wild-type RBD. These data suggest that S100A4 and Rho use different residues to bind the Rhotekin RBD.

To determine whether S100A4, active Rho, and Rhotekin can form a complex, we used a constitutively active L63RhoA to determine if active Rho could co-precipitate Flag RTKN-FL and S100A4. Here, we found that in the presence of calcium GST-L63RhoA precipitates both Flag-RTKN and S100A4 (Fig. 4A lane 6); furthermore, this association of S100A4 with the RhoA-RTKN complex was disrupted by the addition of 5 mM EGTA (lane 8). As expected, however, EGTA did not affect the binding of active Rho to Rhotekin. To confirm the composition of this complex, the L63RhoA pull down assay was performed with control MDA-MB-231 cells or those in which RTKN expression was reduced with RNAi. Here, we found that endogenous S100A4 and Rhotekin precipitated with the constitutively active Rho. Additionally, there was a reduction in the amount of endogenous S100A4 pulled down with GST-L63RhoA in RTKN knockdown cells; and this interaction was calcium-dependent (Fig 4C). In contrast, GST-N19RhoA, a dominant negative Rho, did not pull down either Rhotekin or S100A4 (Fig 4D). Collectively, these data support the formation of a complex comprised of active Rho, Rhotekin, and S100A4.

S100A4 cooperates with Rhotekin to suppress Rho-mediated actin stress fiber formation and promote lamellipodial ruffles in response to EGF

The formation of a RhoA-Rhotekin-S100A4 complex suggests a potential role for this complex in the functional output of Rho signaling. RhoA signaling promotes both actin stress fiber and membrane ruffle formation (10–13) and we find that RhoA is required for MDA-MB-231 cells migration and invasion toward EGF (unpublished data). To confirm

that Rho signaling mediates the formation of membrane ruffles in EGF-stimulated MDA-MB-231 cells, C3 transferase, which inactivates RhoA, B and C by ADP ribosylation, was electroporated into cells prior to treatment with EGF. We found that inhibition of Rho GTPase signaling by C3 impaired membrane ruffling and cortical F-actin bundles in EGF-stimulated MDA-MB-231 cells (supplemental Figure S1). Similar morphological changes were seen with the ROCK inhibitor Y27632 in terms of loss of membrane ruffles, lamellae and contractile actin filaments; however, with the ROCK inhibitor, cells were more elongated (data not shown).

To determine the contribution of the S100A4 and Rhotekin interaction to the organization of the actin cytoskeleton, we created stable transfectants of MDA-MB-231 cells that express either a non-targeting shRNA (shNT) or one targeting S100A4 (shS100A4). These cells were treated with either siRNA targeting Rhotekin (siRtkn) or a non-targeting siRNA (siNT) and changes in F-actin organization were assessed following EGF-stimulation. As shown in Figure 5A, EGF-stimulated MDA-MB-231 cells formed large lamellae with prominent actin-rich lamellipodial ruffles, which were often contiguous over a large portion of the cell periphery (quantified in panels 5E as “many”). Within the body of the cell, thick F-actin fibers, which might be loosely referred to as stress fibers, are seen in low abundance (< 10 per cell) if noted at all. However, when Rhotekin expression is reduced by siRNA, the presence of these F-actin bundles increases in number (> 20 per cell; quantified as “many”) and thickness, but there is little effect on lamellipodial ruffles (Fig. 5B). In contrast, when S100A4 expression is repressed, lamellipodial ruffles become less prominent (referred to as “few” or none when completely absent) and F-actin in the lamellipodium is generally reduced to focal points of polymerization (Fig. 5C, black arrowheads). Furthermore, as seen with Rhotekin knockdown, reduction of S100A4 expression led to an increase in the number of F-actin fibers in the cell body, although these fibers are generally much thinner and more numerous than those seen in the cells with Rhotekin knockdown only (Fig. 5C). These characteristics, quantified in panels 5E and 5F, were more dramatic when both S100A4 and Rhotekin expression were reduced (Fig. 5D) in which, F-actin fibers become much thicker and abundant while lamellipodial ruffles are lost. These data demonstrate cooperation between S100A4 and Rhotekin signaling.

S100A4 and Rhotekin converge on the spatial regulation of myosin light chain phosphorylation

One of the intracellular functions of S100A4 is to prevent the oligomerization of myosin IIA heavy chain (6). Rho acting through ROCK contributes to the activation of myosins through the enhanced phosphorylation of myosin light chain (MLC) through the inhibition of myosin light chain phosphatase. To determine if myosin and MLC might be a convergence point for the S100A4-Rhotekin-Rho complex, we investigated MLC phosphorylation as a readout of this potential cross talk. Using the control and RNAi-mediated S100A4/Rhotekin double knockdown cells, we observed no difference in total MLC phosphorylation determined by immunoblot analysis of whole cell lysates with or without growth factor stimulation (see Supplemental Figure S2). Similarly, we found that the reduction of S100A4 and/or Rhotekin expression did not affect the amount of active RhoA in EGF-stimulated MDA-MB-231 cells

(data not shown). These observations indicate that S100A4 and Rhotekin affect Rho signaling by altering Rho function spatially.

To determine if MLC phosphorylation is altered in a spatial fashion, EGF-stimulated cells were stained for phospho-MLC (pMLC) and F-actin, and then imaged by TIRF microscopy. As shown in Figure 6A, control cells display broad lamellae rich with punctate pMLC staining. At the very leading edge of the lamellipodium of these cells, beneath the membrane ruffles, the pMLC staining present is no longer punctate, but predominantly diffuse in nature (Fig. 6A, inset of middle panel). In cells depleted for Rhotekin, diffuse pMLC staining is also seen where lamellipodial ruffles exist and punctate pMLC associates with thicker actin filaments. In cells depleted for S100A4, this diffuse pMLC staining present in the control cells is notably absent (Fig. 6C and D, insets in middle panels). When either Rhotekin or S100A4 is reduced by RNAi (Fig. 6B–D, middle panels), pMLC puncta become more prominent within the cell body and line up along stress fibers. These data suggest that the interaction of S100A4 and Rhotekin spatially regulates Rho and, therefore, affects the functional output of Rho signaling.

S100A4 cooperates with Rhotekin to promote invasive growth of MDA-MB-231 cells in three-dimensional culture

While RhoA contributes to lamellae and lamellipodia formation and migration in two-dimensions, the contribution of RhoA to tumor invasion is manifested more fully in 3D invasion, as seen specifically with the MDA-MB-231 cells (28, 29). For these experiments, Rhotekin and S100A4 in MDA-MB-231 cells were reduced by RNAi and invasive growth was assessed after four days in Matrigel. As shown in Figure 7A, control cells displayed aggressive invasive growth with “spider-like” protrusions extending into the Matrigel. Reduction of Rhotekin expression did not show a significant effect on the percentage of colonies exhibiting invasive growth, but compared to control cells, the protrusions were much shorter. In cells with reduced S100A4, there was a dramatic decrease in the percentage of colonies showing invasive growth. Interestingly, depletion of both proteins resulted in a more dramatic phenotype; most colonies were smaller with no invasive growth. As shown in Figure 7B, F-actin staining verified that control cells displayed actin-rich projections, and that the F-actin was distributed in the cell periphery. In contrast, knockdown of S100A4 and/or Rhotekin resulted in rounded colonies with minimal projections and F-actin localized at cell-cell junctions. These effects were quantified as shown in Figure 7C. These studies demonstrate that S100A4 and Rhotekin function cooperatively to elicit an invasive morphological phenotype in breast tumor cells.

DISCUSSION

While RhoA is best recognized for its ability to promote stress fiber formation (8), several studies also show that RhoA can specifically promote membrane ruffling and facilitate cell motility, especially in cells of epithelial origin (10–13). To support its role in membrane ruffling, there are substantial data indicating that RhoA is active at the leading edge of migrating cells (9). Definitive evidence was finally presented with the advent of FRET-based reporter of RhoA activity which showed that RhoA activity localizes to sites of active

protrusion and precedes the activation of Rac and cdc42 (30). This occurs not only in fibroblasts (31), but also in cells of epithelial origin where RhoA activation promotes the formation of membrane ruffles (13).

However, a major question has remained: how does RhoA promote lamellae and lamellipodia formation? It is tempting to speculate simply that the choice of one effector controls the switch between Rho's ability to promote membrane ruffles and lamellae in lieu of stress fibers. However, both membrane ruffle and stress fiber formation are mediated through the same Rho effectors, ROCK and mDia (23). The Rho-ROCK pathway inhibits myosin light chain phosphatase, resulting in increased myosin light chain phosphorylation. Phosphorylation of myosin light chain enhances myosin II contractility, which is inhibitory to membrane protrusive activities (32). Therefore, if Rho contributes to lamellipodial protrusions, it is necessary to temper the contractile functions of Rho to facilitate the actin polymerization and membrane protrusion activities of effectors such as mDia (23) and ROCK substrates such as Adducin (10). Here, we provide evidence that the interaction of Rhotekin and S100A4 provide the mechanism for Rho to switch from stress fiber formation to lamellipodial ruffles.

Rhotekin was initially identified as a putative target for Rho (16) and has since been shown to bind multiple proteins involved in cell polarity, focal adhesion, and septin organization (17–19). One recent study showed that Rhotekin is a substrate of protein kinase D and that Rhotekin phosphorylation regulates Rho activity in fibroblasts (33). However, the role of Rhotekin in signaling downstream of Rho remains largely unknown. In our study, we find that Rhotekin interacts with S100A4 and this interaction is mediated through direct, calcium-dependent binding of S100A4 to the RBD of Rhotekin. We also demonstrate that the cooperative signaling between S100A4 and Rhotekin promotes membrane ruffling in EGF-stimulated MDA-MB-231 cells while suppressing stress fiber formation. In addition, we discovered that Rhotekin, S100A4 and active Rho form a complex, thus suggesting that the interaction of Rhotekin and S100A4 facilitates the recruitment of S100A4 to active RhoA. These interesting findings put S100A4 in a position to influence Rho signaling and potentially alter the signaling output of Rho.

S100A4 functions intracellularly by binding to cytoskeletal proteins such as tropomyosin and non-muscle myosin IIA. Notably, myosin II is critical for the migratory process and is a convergence point for small GTPase signaling (32). Myosin IIA, specifically, functions predominantly at the leading edge where myosin light chains are preferentially phosphorylated downstream of RhoA signaling (34). S100A4 binding inhibits myosin-IIA oligomerization and thereby limits the contractile functions of this molecule (35). If S100A4 restricts myosin-IIA contractility, coupling Rho signaling to S100A4 through Rhotekin at the leading edge of cells would limit contractility in a spatial and temporal manner, and thus permit the protrusive effects of Rho signaling to dominate. Notably, one of the reported roles of S100A4 in cell motility is to control the localization and stability of cellular protrusions (7). Therefore, the coupling of S100A4 to RhoA would increase the efficiency of generating forward protrusions and enhancing directed cell motility.

These observations and concepts led us to the molecular model depicted in Figure 8, which helps to explain how the interaction of S100A4 and Rhotekin lead to a functional switch in Rho function. When both Rhotekin and S100A4 are expressed, growth factor stimulation of Rho activity leads to the coupling of Rho to S100A4. Under these conditions, myosin II oligomerization is restricted in close proximity to active Rho, thus limiting stress fiber formation. The inhibition of myosin-mediated actin contractility then permits membrane ruffling and lamellae formation to predominate downstream of Rho effectors such as ROCK (Fig. 8A). When Rhotekin is absent, S100A4 and Rho are uncoupled. Under this condition, Rho activation is not restricted to the leading edge, which allows for the formation of membrane ruffles at the leading edge and stress fibers in the cell body (Fig. 8B). This concept is supported by the presence of both membrane ruffles and stress fibers with RNAi-mediated reduction in Rhotekin (Fig. 5B) and the altered distribution of pMLC (Fig. 6). Without S100A4, membrane ruffles are unable to form (Fig. 5C) due to the increase in oligomeric myosin and absence of monomeric myosin at the leading edge (Fig. 6). Notably, the loss of both S100A4 and Rhotekin exacerbates the thickness and number of stress fibers.

Lastly, we find that S100A4 cooperates with Rhotekin to promote invasive growth in 3D culture. Tumor invasive growth is defined as a complex, multistep program involved in the interplay of tumor cells and the microenvironment, and in turn tumor cells acquire the propensity for migration, invasion, and proliferation (36). Interestingly, a recent study suggested that both intracellular and extracellular S100A4 affect TGFα-mediated branching phenotype of normal mammary gland (37). We cannot discount that signal relay from secreted S100A4 contributes to promoting invasive growth considering the duration (four days) of these assays. However, our short-term studies demonstrate that S100A4 and Rhotekin function cooperatively to elicit the same morphological phenotypes in breast tumor cells, consistent with an intracellular role for S100A4 as a major contributor to this phenotype.

Mechanisms governing carcinoma cells in 3D and *in vivo* can differ substantially from those in two-dimensional (2D) culture systems (38). However, in both 2D and 3D systems, polarization through the formation of lamellae or pseudopodia is important for migration and invasion. Previous work in breast cancer highlights the importance of lamellae formation and directed migration in promoting carcinoma metastasis where cells that can polarize toward blood vessels through lamellae formation are more metastatic and those that cannot (39, 40). Not only does RhoA have the potential to contribute to lamellae formation, it has been demonstrated that RhoA activity can be spatially regulated during cell invasion in live animals, as shown in pancreatic cancer (41). Considering the mounting evidence that RhoA plays a critical role in the migration, invasion and metastasis of various types of carcinomas (23, 42, 43), better insight into how RhoA contributes to these processes and whether the cooperative signaling between Rhotekin and S100A4 affects Rho spatially in a 3D culture system will be an important avenue of investigation for future studies.

In summary, we identified a novel interaction between the pro-metastatic protein S100A4 and the Rho effector Rhotekin. This coupling of S100A4 to Rhotekin permits S100A4 to complex with RhoA and switch Rho function from stress fiber formation to membrane ruffling. We propose that the S100A4/Rhotekin interaction changes Rho signaling outcome

by affecting how Rho assembles and modifies the actin cytoskeleton spatially. Moreover, S100A4 and Rhotekin cooperate to confer an invasive tumor phenotype in breast cancer cells through its ability to promote membrane protrusions and invasive growth.

MATERIALS AND METHODS

Cell lines and plasmids

MDA-MB-231 and HeLa cells were cultured and transfected with select cDNAs or siRNAs (Dharmacon/Fisher) as described previously (44, 45). Flag- and myc-tagged Rhotekin constructs (46) were obtained from Dr. Kohichi Nagata (Institute for Developmental Research, Alchi Human Service Center, Alchi, Japan). Plasmids pGEX-4T-1-mouse mDia RBD, pGEX-4T-3-mouse ROCK-II RBD and pGEX-mouse citron RBD were obtained from Dr. Shuh Narumiya (Kyoto University Faculty of Medicine, Japan). GST-RBD-AAA (27) was obtained from Dr. G. Steven Martin (University of California, Berkeley). pGEX-L63RhoA was obtained from Dr. Keith Burridge (University of North Carolina-Chapel Hill)

For construction of the HA-RTKN-FL plasmid, mouse cDNA was used as the template to amplify the full-length RTKN using specific primers (forward, 5′ GCG-ATA-TCA-CAG-ATT-GCG-CAT-CCT-GGA 3′; reverse, 5′ GCT-CTA-GAT-GAC-TTC-ATC-ACA-ACA-GTG-CCT 3′) and inserted into EcoR V and Xba I sites of pcDNA3.1-HA vector. For construction of GST-Rhophilin2-RBD and GST-PKN1-RBD, cDNA from MDA-MB-435 cells was used as the template to amplify RBDs using isoform specific primers for PKN1 (forward, 5′ CGG-GAT-CCC-AGA-GTG-AGC-CTC-GCA-GCT-GGT-CC 3′; reverse, 5′ CCG-CTC-GAG-GGG-AAG-CAC-CAC-GTG-GGC-GT 3′) and Rhophilin 2, (forward, 5′ CGG-GAT-CCC-AGC-CGC-TGG-AGA-AGG-AGA-A 3′ and reverse, 5′ CGG-CTC-GAG-GCA-TCT-GCA-GGT-CTG-AGT-TGA-CG 3′). PCR products were inserted into the BamH I and Xho I sites of pGEX-6P-3 vector. GST-N19RhoA was generated by sub-cloning from myc-N19RhoA construct as described previously (47) and inserting into the Xho I and EcoR I sites of pGEX-6P-3 vector. All plasmids were confirmed by sequencing.

Lentivirus-mediated shRNA constructs (targeting sequence: 5′ CGC-CAT-GAT-GTG-TAA-CGA-ATT 3′; Sigma) were used to generate stable reduction of S100A4 expression in MDA-MB-231 cells.

RhoA activity, GST-fusion protein binding, and immunoprecipitation assays

RhoA activity was assessed with the Rhotekin binding assay as described previously (12, 44, 47). The expression of the GST-RBDs from different Rho effectors, GST, GST-L63RhoA and GST-N19RhoA were induced by 1mM IPTG in BL21 bacteria and coupled to Glutathione Sepharose 4B beads (GE healthcare). Then GST-fusion protein binding and immunoprecipitation assays were carried out in lysis buffer (50 mM Tris, pH 7.2, 500 mM NaCl, 1% Triton X-100, 0.25% sodium deoxycholate, 0.1% SDS, 10 mM $MgCl_2$, 2 mM $CaCl_2$, 10 μg/ml protease inhibitor cocktail (48), and 1 mM PMSF). GST-fusion protein coupled beads (35μl) were incubated with cell lysates or purified S100A4 for 30 mins at 4°C. For immunoprecipitation of tagged proteins, 10 μl of anti-c-myc coupled agarose beads (clone 9E10, Santa Cruz Biotechnology) and 1 μg monoclonal anti-Flag (clone M2, Sigma)

were incubated with precleared cell lysates at 4°C overnight. Beads were then rinsed 3 times with wash buffer (50 mM Tris, pH 7.2, 150 mM NaCl, 1% Triton X-100, 10 mM $MgCl_2$, plus protease inhibitors). The GST-beads coupled proteins and immunoprecipitated proteins complexes were resuspended in 2X Laemmli sample buffer, separated by SDS-PAGE and immunoblotted as indicated. Human S100A4 was expressed and purified as described previously (7, 49).

Immunocytochemistry staining and imaging

Cells (2.5×10^4)from noted treatments were seeded on glass coverslips coated with 50 μg/ml collagen I (BD Bioscience) for 2 hrs, and then treated with 5 ng/ml EGF (Pepro Tech) for 5 mins. Cells were fixed, permeabilized, and immunostained as described previously (12, 50) using the following antibodies: anti-S100A4 (1:400, Dako), anti-pMLC (S19, 1:100, Cell Signaling), HA-probe (F-7, 1:100, Santa Cruz), Alexa Fluor 488 goat anti-rabbit IgG (Molecular Probes) or Cy3-conjugated donkey anti-mouse IgG (Jackson Immune Research). TRITC-Phalloidin (Sigma) was used to stain F-actin. Coverslips were mounted in VECTASHIELD mounting medium for fluorescence (Vector Laboratories, Inc). Confocal images were captured on an Olympus FV1000 confocal microscope using an Olympus 60X UPlanS Apo NA 1.35 oil objective and Olympus FV10-ASW2 software. TIRF microscopy was performed using a Nikon Eclipse Ti-E TIRF microscope equipped with a 60X, 1.45 NA objective, CoolSNAP HQ2 CCD camera (Roper Scientific). These images were acquired at room temperature and analyzed by using NIS-Elements (Nikon). Image quality in terms of subtracted background and input intensity range was optimized in NIS-Elements using the automated look-up tables under linear settings (1.0 gamma setting). Images were cropped in Adobe Photoshop and assembled in Adobe Illustrator CS5.

Three-dimensional culture

MDA-MB-231 cells were grown in three-dimensional culture as described previously to assess invasive growth (51). Briefly, cells (5×10^3) in 200 μl DMEM/F12 plus 1% FBS were seeded onto solidified growth factor reduced Matrigel (BD Biosciences; 100 μl per well of 8-well chamber slide) and then covered with 10% Matrigel containing medium. After 3 days, 8 representative fields for each condition were assessed for the percentage of colonies demonstrating invasive growth. Then 20 μl of Matrigel containing colonies were smeared onto a slide, fixed with 4% paraformaldehyde, permeabilized and immunostained as described above.

Supplementary Material

Refer to Web version on PubMed Central for supplementary material.

Acknowledgments

We thank Dr. Ren Xu for his kind aid with 3D culture related experiments; Dr. Jianhang Jia for assistance with the confocal microscopy analysis; Drs. Tianyan Gao and Jianyu Liu for reagents and technical support for generating shRNA stable cell line; Drs. Kohich Nagata, Shuh Narumiya and G. Steven Martin for reagents; Dr. Juanjuan Yang for validating select data; and Diane Wright for assistance with graphics. This work was supported with National Institutes of Health grants CA109136 (KLO) and CA129598 (ARB).

Abbreviations

shNT	non-targeting shRNA
siNT	non-targeting siRNA
PBD	Pak Rac/Cdc42 binding domains
RBD	Rho binding domain

REFRENCES

1. Garrett SC, Varney KM, Weber DJ, Bresnick AR. S100A4, a mediator of metastasis. J Biol Chem. 2006; 281(2):677–80. [PubMed: 16243835]
2. Takenaga K, Nakanishi H, Wada K, Suzuki M, Matsuzaki O, Matsuura A, et al. Increased expression of S100A4, a metastasis-associated gene, in human colorectal adenocarcinomas. Clin Cancer Res. 1997; 3(12 Pt 1):2309–16. [PubMed: 9815629]
3. Rudland PS, Platt-Higgins A, Renshaw C, West CR, Winstanley JH, Robertson L, et al. Prognostic significance of the metastasis-inducing protein S100A4 (p9Ka) in human breast cancer. Cancer Res. 2000; 60(6):1595–603. [PubMed: 10749128]
4. Boye K, Maelandsmo GM. S100A4 and metastasis: a small actor playing many roles. Am J Pathol. 2010; 176(2):528–35. [PubMed: 20019188]
5. Kim EJ, Helfman DM. Characterization of the metastasis-associated protein, S100A4. Roles of calcium binding and dimerization in cellular localization and interaction with myosin. J Biol Chem. 2003; 278(32):30063–73. [PubMed: 12756252]
6. Li Z-H, Spektor A, Varlamova O, Bresnick AR. Mts1 regulates the assembly of nonmuscle myosin-IIA. Biochemistry. 2003; 42(48):14258–66. [PubMed: 14640694]
7. Li ZH, Bresnick AR. The S100A4 metastasis factor regulates cellular motility via a direct interaction with myosin-IIA. Cancer Res. 2006; 66(10):5173–80. [PubMed: 16707441]
8. Hall A. The cytoskeleton and cancer. Cancer Metastasis Rev. 2009; 28(1–2):5–14. [PubMed: 19153674]
9. Spiering D, Hodgson L. Dynamics of the Rho-family small GTPases in actin regulation and motility. Cell Adh Migr. 2011; 5(2):170–80. [PubMed: 21178402]
10. Fukata Y, Oshiro N, Kinoshita N, Kawano Y, Matsuoka Y, Bennett V, et al. Phosphorylation of adducin by Rho-kinase plays a crucial role in cell motility. J Cell Biol. 1999; 145(2):347–61. [PubMed: 10209029]
11. Nishiyama T, Sasaki T, Takaishi K, Kato M, Yaku H, Araki K, et al. *rac* p21 is involved in insulin-induced membrane ruffling and *rho* p21 is involved in hepatocyte growth factor- and 12-0-tetradecanoylphorbol-13-acetate (TPA)-induced membrane ruffling in KB cells. Mol Cell Biol. 1994; 14(4):2247–456.
12. O'Connor KL, Nguyen B-K, Mercurio AM. RhoA function in lamellae formation and migration is regulated by the α6β4 integrin and cAMP. J Cell Biol. 2000; 148(2):253–8. [PubMed: 10648558]
13. Kurokawa K, Matsuda M. Localized RhoA activation as a requirement for the induction of membrane ruffling. Mol Biol Cell. 2005; 16(9):4294–303. [PubMed: 15987744]
14. Watanabe N, Kato T, Fujita A, Ishizaki T, Narumiya S. Cooperation between mDia1 and ROCK in Rho-induced actin reorganization. Nat Cell Biol. 1999; 1(3):136–43. [PubMed: 10559899]
15. Tsuji T, Ishizaki T, Okamoto M, Higashida C, Kimura K, Furuyashiki T, et al. ROCK and mDia1 antagonize in Rho-dependent Rac activation in Swiss 3T3 fibroblasts. J Cell Biol. 2002; 157(5): 819–30. [PubMed: 12021256]
16. Reid T, Furuyashiki T, Ishizaki T, Watanabe G, Watanabe N, Fujisawa K, et al. Rhotekin, a new putative target for Rho bearing homology to a serine/threonine kinase, PKN, and rhophilin in the rho-binding domain. J Biol Chem. 1996; 271(23):13556–60. [PubMed: 8662891]

17. Nagata K, Ito H, Iwamoto I, Morishita R, Asano T. Interaction of a multi-domain adaptor protein, vinexin, with a Rho-effector, Rhotekin. Med Mol Morphol. 2009; 42(1):9–15. [PubMed: 19294487]
18. Sudo K, Ito H, Iwamoto I, Morishita R, Asano T, Nagata K. Identification of a cell polarity-related protein, Lin-7B, as a binding partner for a Rho effector, Rhotekin, and their possible interaction in neurons. Neurosci Res. 2006; 56(4):347–55. [PubMed: 16979770]
19. Ito H, Iwamoto I, Mizutani K, Morishita R, Deguchi T, Nozawa Y, et al. Possible interaction of a Rho effector, Rhotekin, with a PDZ-protein, PIST, at synapses of hippocampal neurons. Neurosci Res. 2006; 56(2):165–71. [PubMed: 16934893]
20. Ying-Tao Z, Yi-Ping G, Lu-Sheng S, Yi-Li W. Proteomic analysis of differentially expressed proteins between metastatic and non-metastatic human colorectal carcinoma cell lines. Eur J Gastroenterol Hepatol. 2005; 17(7):725–32. [PubMed: 15947549]
21. Liu CA, Wang MJ, Chi CW, Wu CW, Chen JY. Rho/Rhotekin-mediated NF-kappaB activation confers resistance to apoptosis. Oncogene. 2004; 23(54):8731–42. [PubMed: 15480428]
22. Fujisawa K, Madaule P, Ishizaki T, Watanabe G, Bito H, Saito Y, et al. Different regions of Rho determine Rho-selective binding of different classes of Rho target molecules. J Biol Chem. 1998; 273(30):18943–9. [PubMed: 9668072]
23. Narumiya S, Tanji M, Ishizaki T. Rho signaling, ROCK and mDia1, in transformation, metastasis and invasion. Cancer Metastasis Rev. 2009; 28(1–2):65–76. [PubMed: 19160018]
24. Bishop AL, Hall A. Rho GTPases and their effector proteins. Biochem J. 2000; 348(Pt 2):241–55. [PubMed: 10816416]
25. Liu CA, Wang MJ, Chi CW, Wu CW, Chen JY. Overexpression of rho effector rhotekin confers increased survival in gastric adenocarcinoma. J Biomed Sci. 2004; 11(5):661–70. [PubMed: 15316142]
26. Garrett SC, Varney KM, Weber DJ, Bresnick AR. S100A4, a mediator of metastasis. J Biol Chem. 2006; 281(2):677–80. [PubMed: 16243835]
27. Berdeaux RL, Diaz B, Kim L, Martin GS. Active Rho is localized to podosomes induced by oncogenic Src and is required for their assembly and function. J Cell Biol. 2004; 166(3):317–23. [PubMed: 15289494]
28. Pillé JY, Denoyelle C, Varet J, Bertrand JR, Soria J, Opolon P, et al. Anti-RhoA and anti-RhoC siRNAs inhibit the proliferation and invasiveness of MDA-MB-231 breast cancer cells in vitro and in vivo. Mol Ther. 2005; 11(2):267–74. [PubMed: 15668138]
29. Wu D, Asiedu M, Wei Q. Myosin-interacting guanine exchange factor (MyoGEF) regulates the invasion activity of MDA-MB-231 breast cancer cells through activation of RhoA and RhoC. Oncogene. 2009; 25(22):2219–30. [PubMed: 19421144]
30. Machacek M, Hodgson L, Welch C, Elliott H, Pertz O, Nalbant P, et al. Coordination of Rho GTPase activities during cell protrusion. Nature. 2009; 461(7260):99–10. [PubMed: 19693013]
31. Pertz O, Hodgson L, Klemke RL, Hahn KM. Spatiotemporal dynamics of RhoA activity in migrating cells. Nature. 2006; 440(7087):1069–72. [PubMed: 16547516]
32. Vicente-Manzanares M, Ma X, Adelstein RS, Horwitz AR. Non-muscle myosin II takes centre stage in cell adhesion and migration. Nat Rev Mol Cell Biol. 2009; 10:778–90. [PubMed: 19851336]
33. Pusapati GV, Eiseler T, Rykx A, Vandoninck S, Derua R, Waelkens E, et al. Protein Kinase D regulates RhoA activity via Rhotekin phosphorylation. J Biol Chem. 2012; 287(12):9473–83. [PubMed: 22228765]
34. Sandquist JC, Swenson KI, Demali KA, Burridge K, Means AR. Rho kinase differentially regulates phosphorylation of nonmuscle myosin II isoforms A and B during cell rounding and migration. J Biol Chem. 2006; 281(47):35873–83. [PubMed: 17020881]
35. Li ZH, Dulyaninova NG, House RP, Almo SC, Bresnick AR. S100A4 regulates macrophage chemotaxis. Mol Biol Cell. 2010; 21(15):2598–610. [PubMed: 20519440]
36. Trusolino L, Comoglio PM. Scatter-factor and semaphorin receptors: cell signalling for invasive growth. Nat Rev Cancer. 2002; 2(4):289–300. [PubMed: 12001990]

37. Andersen K, Mori H, Fata J, Bascom J, Oyjord T, Maelandsmo GM, et al. The metastasis-promoting protein S100A4 regulates mammary branching morphogenesis. Dev Biol. 2011; 352(2): 181–90. [PubMed: 21195708]
38. Friedl P, Wolf K. Plasticity of cell migration: a multiscale tuning model. J Cell Biol. 2009; 188(1): 11–9. [PubMed: 19951899]
39. Condeelis JS, Wyckoff JB, Bailly M, Pestell R, Lawrence D, Backer J, et al. Lamellipodia in invasion. Semin Cancer Biol. 2001; 11:119–28. [PubMed: 11322831]
40. Wyckoff JB, Jones JG, Condeelis JS, Segall JE. A critical step in metastasis: in vivo analysis of intravasation at the primarytumor. Cancer Res. 2000; 60:2504–11. [PubMed: 10811132]
41. Timpson P, McGhee EJ, Morton JP, von Kriegsheim A, Schwarz JP, Karim SA, et al. Spatial regulation of RhoA activity during pancreatic cancer cell invasion driven by mutant p53. Cancer Res. 2011; 71(3):747–57. [PubMed: 21266354]
42. Vega FM, Ridley AJ. Rho GTPases in cancer cell biology. FEBS Lett. 2008; 82(14):2093–101. [PubMed: 18460342]
43. Zhao X, Lu L, Pokhriyal N, Ma H, Duan L, Lin S, et al. Overexpression of RhoA induces preneoplastic transformation of primary mammary epithelial cells. Cancer Res. 2009; 69(2):483–91. [PubMed: 19147561]
44. Chen M, Towers LN, O'Connor KL. LPA2 (EDG4) mediates Rho-dependent chemotaxis with lower efficacy than LPA1 (EDG2) in breast carcinoma cells. Am J Physiol Cell Physiol. 2007; 292(5):C1927–33. [PubMed: 17496233]
45. Chen M, Sinha M, Luxon BA, Bresnick AR, O'Connor KL. Integrin alpha6beta4 controls the expression of genes associated with cell motility, invasion, and metastasis, including S100A4/metastasin. J Biol Chem. 2009; 284(3):1484–94. [PubMed: 19011242]
46. Ito H, Iwamoto I, Morishita R, Nozawa Y, Narumiya S, Asano T, et al. Possible role of Rho/Rhotekin signaling in mammalian septin organization. Oncogene. 2005; 24(47):7064–72. [PubMed: 16007136]
47. O'Connor KL, Chen M, Towers LN. Integrin α6β4 cooperates with LPA signaling to stimulate Rac through AKAP-Lbc-mediated RhoA activation. Am J Physiol Cell Physiol. 2012; 302(3):C605–14. [PubMed: 22049212]
48. Kelloff GJ, Lubet RA, Fay JR, Steele VE, Boone CW, Crowell JA, et al. Farnesyl protein transferase inhibitors as potential cancer chemopreventives. Cancer Epidemiol Biomarkers Prev. 1997; 6(4):267–82. [PubMed: 9107432]
49. Vallely KM, Rustandi RR, Ellis KC, Varlamova O, Bresnick AR, Weber DJ. Solution structure of human Mts1 (S100A4) as determined by NMR spectroscopy. Biochemistry. 2002; 41(42):12670–80. [PubMed: 12379109]
50. O'Connor KL, Shaw LM, Mercurio AM. Release of cAMP gating by the α6β4 integrin stimulates lamellae formation and the chemotactic migration of invasive carcinoma cells. J Cell Biol. 1998; 143:1749–60. [PubMed: 9852165]
51. Xu R, Spencer VA, Bissell MJ. Extracellular matrix-regulated gene expression requires cooperation of SWI/SNF and transcription factors. J Biol Chem. 2007; 282(20):14992–9. [PubMed: 17387179]

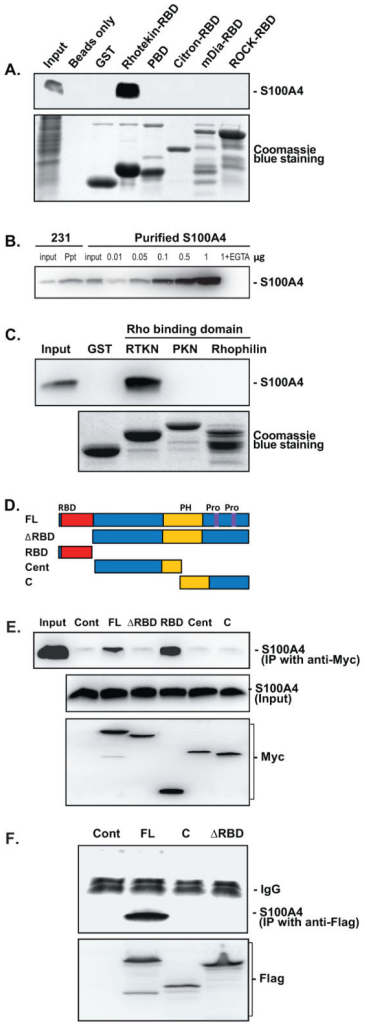

Figure 1. S100A4 binds to Rhotekin but not the other Rho effectors in a calcium-dependent manner

(A) GST-fusion proteins of different Rho effector RBDs were purified, coupled to glutathione beads and incubated with cell lysates from MDA-MB-231 cells, as noted. Beads were then washed and S100A4 content assessed by immunoblot analysis using 10% of the cell lysate as input control (top panel). Equal quantities of each fusion protein were separated by 10% SDS-PAGE followed by Coomassie blue staining (bottom panel). (B) Varying amounts of purified S100A4 were incubated with Rhotekin RBD-glutathione beads in the presence calcium or 5 mM EGTA, washed and immunoblotted for S100A4. Input = 10 ng S100A4. MDA-MB-231 lysate input and Rhotekin RBD precipitates (Ppt) represent positive controls. (C) GST fusion proteins of RBDs from class I Rho effectors, as indicated, or GST alone were purified, coupled to glutathione beads and incubated with 100 ng purified S100A4. Beads were then washed and associated proteins immunoblotted for S100A4 (top panel). Fusion protein content on beads was assessed as in (A) (bottom panel). 10 ng purified S100A4 was used as the input. (D) Domain structure of Rhotekin constructs used in (E) and (F). (E) MDA-MB-231 cells were transfected with myc-RTKN-FL, -ΔRBD, -RBD, -Cent, and C-terminus constructs or empty vector (Control). After 48 hrs, cells were

lysed and immunoprecipitation assays were performed followed by immunoblotting for S100A4 (E, top panel for IP and middle panel for input) and anti-myc (bottom panel). (F) MDA-MB-231 cells were transfected with Flag-RTKN-FL, C-terminus, and -ΔRBD constructs or empty vector (Control). After 48 hrs, cells were lysed and immunoprecipitation assays were performed followed by immunoblotting for S100A4 (top panel) and Flag (bottom panel).

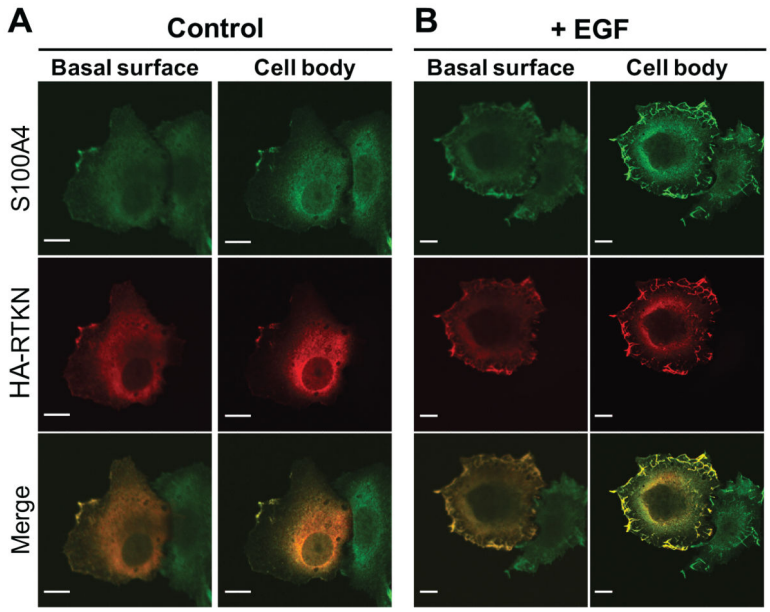

Figure 2. S100A4 and Rhotekin colocalize at the leading edge of migrating cells

HeLa cells, which express endogenous S100A4, were transfected with HA-RTKN-FL. After 48 hrs, suspended cells (2.5×10^4) were seeded on glass coverslips coated with 50 μg/ml collagen I in serum-free medium for 2 hrs before treatment with BSA (A) or EGF (5 ng/ml; B) for 5 mins. Cells were fixed and immunostained for S100A4 (green) and HA (red). Images were taken every 0.5 μm starting from the basal surface. The representative images from one of three separate experiments are shown. For each condition, images from both basal surface and 1.5 μm up to the basal level (cell body) are depicted, as noted.

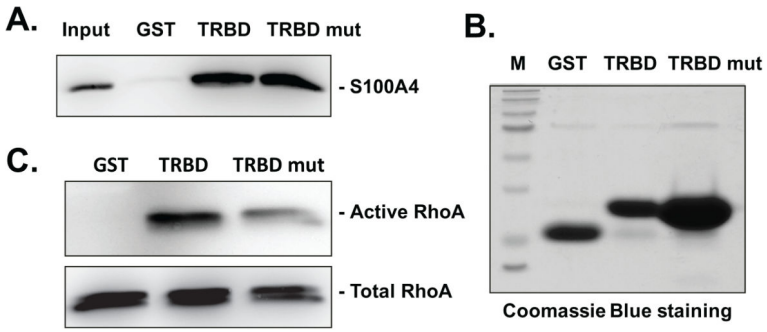

Figure 3. S100A4 and RhoA bind different residues within the Rhotekin RBD

(A) GST or GST fusion proteins of TRBD and TRBD triple A mutants were purified, coupled to glutathione beads and incubated with 100 ng purified S100A4. Beads were washed and immunoblotted for S100A4. 10 ng purified S100A4 was used as the input control. (B) The same amount of protein coupled beads as used in (A) were separated by 10% SDS-PAGE followed by Coomassie blue staining. (C) RhoA activity assay was performed by using GST or GST-fusion protein coupled beads with cell lysates from MDA-MB-231 cells seeded on collagen I-coated dishes and treated with 100 nM LPA for 5 mins.

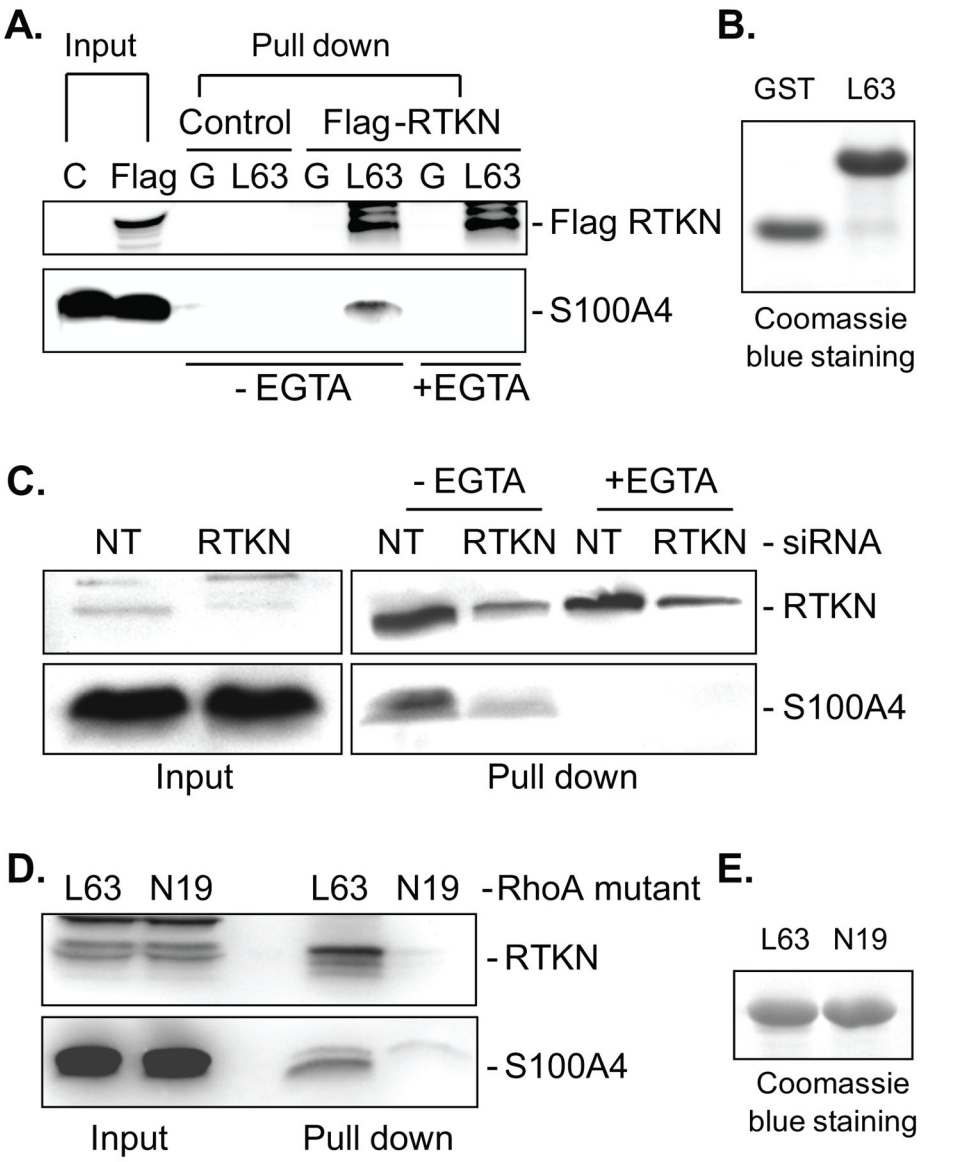

Figure 4. S100A4, Rhotekin, and active Rho form a complex. (A) Flag-RTKN full length was transfected into HeLa cells

After 48 hrs, bacterially-expressed GST or GST-L63RhoA coupled glutathione beads were incubated with cell lysates in the presence of calcium or 5 mM EGTA, as noted, followed by immunoblotting with Flag (top panel) and S100A4 (bottom panel) antibodies. (B) Representative samples of GST and GST-L63RhoA fusion proteins used in the pull down assays analyzed by SDS-PAGE and Coomassie blue staining. (C) MDA-MB-231 cells were electroporated with siRNA targeting Rhotekin (RTKN) or a non-targeting siRNA (NT). After 72 hrs, cells were lysed and incubated with bacterially expressed GST-L63RhoA coupled glutathione beads for 30 mins in the presence of calcium or 5 mM EGTA followed by immunoblotting with Rhotekin or S100A4 antibodies, as indicated. (D) MDA-MB-231 cell lysate was incubated with beads coupled to L63RhoA or N19RhoA. Protein pulled down with beads and lysate input controls (5%) were then immunoblotted for Rhotekin (top

panel) or S100A4 (bottom panel). (E) Coomassie blue staining of representative samples of GST-L63RhoA and GST-N19RhoA fusion proteins used in (D).

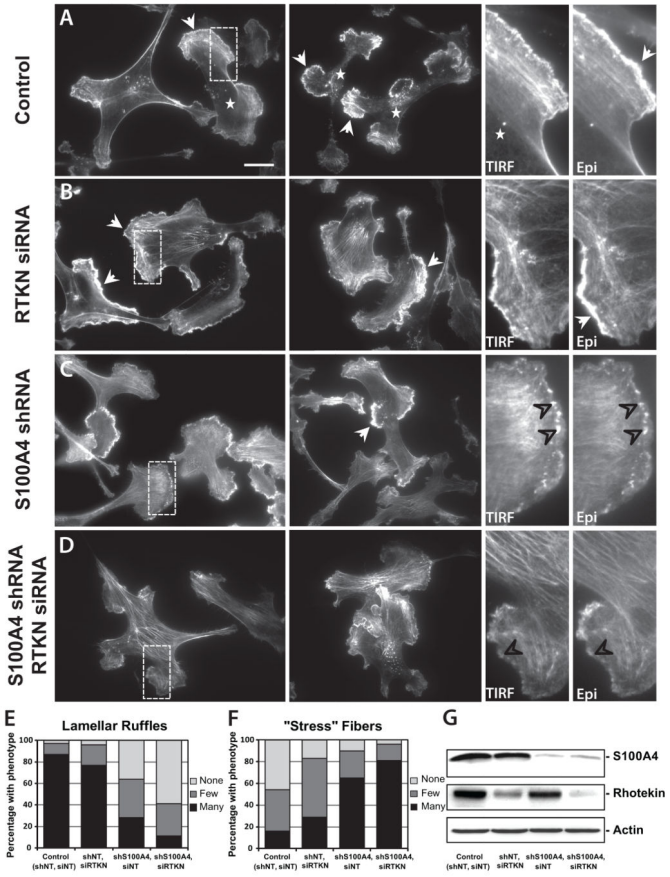

Figure 5. S100A4 and Rhotekin cooperate to suppress actin stress fiber formation and promote membrane ruffle formation in response to EGF

MDA-MB-231 cells were stably transfected with either a non-targeting shRNA (shNT) or one targeting S100A4 (shS100A4). Cells were transiently transfected with siRNA targeting Rhotekin (siRTKN) or a non-targeting siRNA (siNT). After 48 hrs, cells were plated onto collagen-coated coverslips in serum-free medium for 3 hrs before treating with 5 ng/ml EGF for 5 mins. Cells were stained with TRITC-phalloidin and immunostained for S100A4. Cells were imaged using widefield epifluorescence (Epi) and total interference reflection fluorescence (TIRF) microscopy and quantified for the presence of membrane ruffles at the lamellipodium and contractile fibers within the cell body. Representative data are shown for cells transfected with (A) with shNT and siNT (Control); (B) shNT and siRTKN; (C) shS100A4 and siNT; and (D) shS100A4 and siRTKN. Left two panels in (A–D) are representative TIRF images; scale bar in (A) depicts 20 μm for these images. The right two images are higher magnifications of the region highlighted by the rectangular box in the image to the left that were imaged either by TIRF or widefield epifluorescence (Epi), as noted. Arrows (A–C) represent lamellipodial ruffles; stars (A) denote regions devoid of stress fiber-like actin filaments; and black open arrowheads (B, C) show regions of focal actin polymerization which do not result in productive ruffles. (E, F) Quantification of lamellipodial ruffles (E) and notable F-actin fibers (F) present in 100 cells from each condition. (G) Immunoblot analysis of S100A4, Rhotekin and actin expression for cells under each experimental condition.

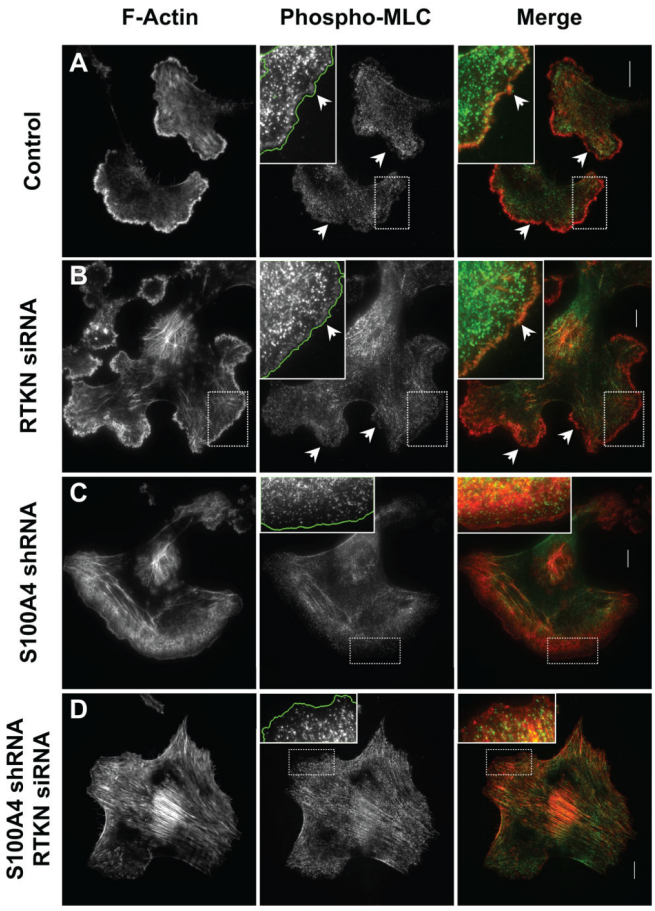

Figure 6. Rhotekin and S100A4 cooperation regulate the spatial distribution of pMLC

MDA-MB-231 cells with RNAi-mediated reduction of S100A4 and/or Rhotekin were plated on collagen-coated coverslips and treated with EGF for 5 mins, as described in Figure 5. Cells were fixed, stained for F-actin (left panels) and pMLC (middle panels), and imaged using TIRF microscopy as described in the Methods section. Representative data are shown for cells transfected with (A) with shNT and siNT (Control); (B) shNT and siRTKN; (C) shS100A4 and siNT; and (D) shS100A4 and siRTKN. Insets represent 4X magnification of area noted by the dashed box in the main middle and right panels, which have been brightened to highlight diffuse pMLC staining of the leading edge in panels A and B and the absence of this staining in panels C and D. Arrows in A and B highlight select spots of diffuse pMLC staining that colocalizes with lamellipodial actin polymerization. The green line in the insets of the middle panels denotes the cell boundaries determined by Region of Interest (ROI) delineation from F-actin images. Scale bars in merged images indicate 10 μm.

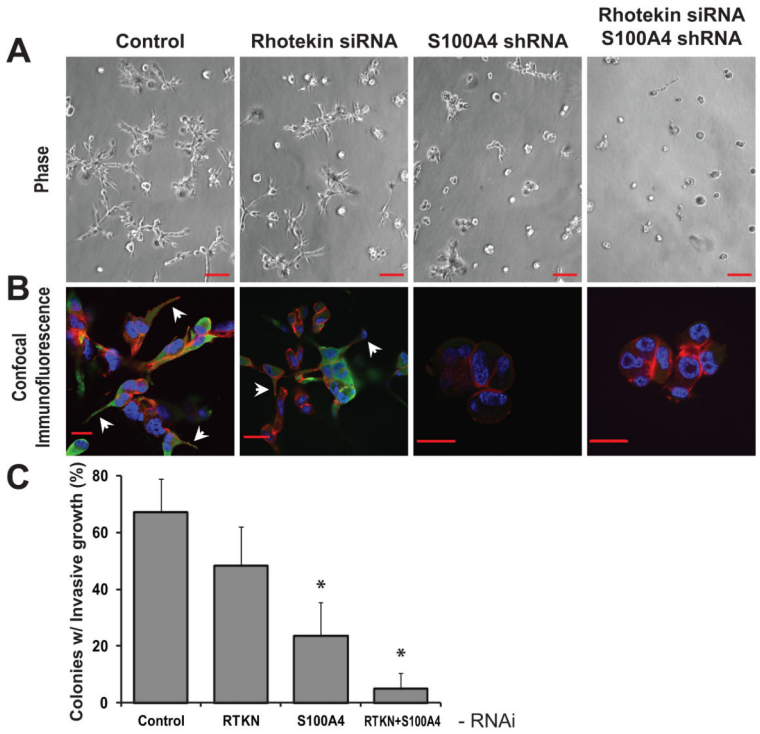

Figure 7. S100A4 and Rhotekin cooperate to promote invasive growth of 3D cultures of MDA-MB-231 cells

(A) Representative phase-contrast images of MDA-MB-231 cells in 3D culture after reduction of S100A4 and/or RTKN expression by RNAi. Scale bars represent a distance of 100 μm. (B) Matrigel containing colonies from cells in (A) were smeared onto slides, fixed, permeabilized, and stained for F-actin (TRITC-phalloidin; red), S100A4 (anti-S100A4; green) and nuclei (DAPI; blue). The arrows indicate invasive cell protrusion into the Matrigel. Scale bars = 20 μm. (C) Quantification of the percentage of colonies with invasive growth from one of at least three representative experiments. Values represent the means ± s.d. from eight fields of 18–40 colonies in each condition (* $p<0.01$ by t-test).

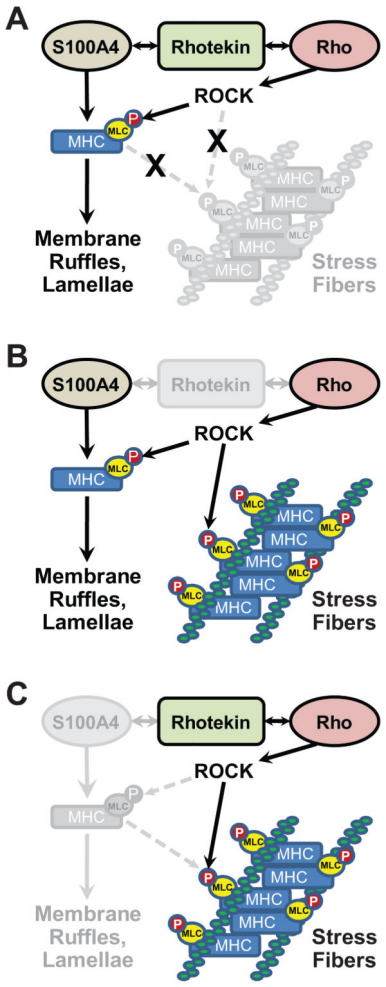

Figure 8. Proposed model of S100A4-Rhotekin cooperation in Rho signaling

(A) We suggest that the coupling of Rho to S100A4 is mediated by Rhotekin. Under this model, we propose that S100A4-mediated inhibition of myosin IIA heavy chain oligomerization limits the contractility of pMLC-myosin IIA complex. Under this condition, the actin polymerization functions of ROCK (shown here) and other effectors such as mDia (not shown) predominate, thus permitting the formation of lamellae. (B) The loss of Rhotekin, uncouples the functions of S100A4 and Rho. At the the leading edge where S100A4 is active, Rho promotes membrane ruffling; in the cell body where S100A4 is not active, Rho stimulates stress fiber formation. (C) In the absence of S100A4, Rho-mediated MLC phosphorylation and mDia activation permit myosin-IIA oligomerization and the contractility required for stress fiber formation; whereas membrane ruffles downstream of RhoA are unable to form. The loss of both S100A4 and Rhotekin augments this phenotype. Components in grey represent inactive pathways.